Proc. Natl. Acad. Sci. USA
Vol. 90, pp. 4191–4195, May 1993
Evolution

Images of evolution: Origin of spontaneous RNA replication waves

(selection/reaction diffusion/fluorescence/bioreactor/Qβ replicase)

J. S. McCaskill* and G. J. Bauer†

Max-Planck-Institut für Biophysikalische Chemie, Nikolausberg am Fassberg, D-3400 Göttingen, Federal Republic of Germany

Communicated by Manfred Eigen, August 19, 1992

ABSTRACT **Self-replicating molecules set up traveling concentration waves that propagate in an aqueous enzyme solution. The velocity of each wave provides an accurate (±0.1%) noninvasive measure of fitness for the RNA species currently growing in its front. Evolution may be followed from changes in the front velocity, and these differ from wave to wave. Thousands of controlled evolution reactions in traveling waves have been monitored in parallel to obtain quantitative images of the stochastic process of natural selection. An RNA polymerase (RNA-dependent RNA nucleotidyltransferase, EC 2.7.7.6), extracted from bacteria infected by the Qβ RNA virus, catalyzes the replication. The traveling waves that arise spontaneously without added RNA provide a model system for major evolutionary change.**

An innovative form of spatially inhomogeneous biochemistry permits the simultaneous observation of >1000 separate evolution processes. As a first result, we were able to resolve a phenomenon of spontaneous creation as a process involving rapid evolution: *de novo* synthesis of self-replicating RNA (1) is shown here to be a statistically reproducible phenomena of natural selection rather than a single enzyme-instructed event. The Qβ replicase enzyme is an RNA polymerase (M_r 215,000, four subunits) isolated from Qβ phage-infected *Escherichia coli* cells (2, 3). The short time (about 30 s) for replication and its kinetically well-characterized mechanism (4–6) make the system an ideal candidate for evolutionary studies. We use massively parallel observations to deal with the stochastic nature of mutational change and to utilize the velocity of traveling concentration waves as an accurate noninvasive measure of fitness.

The process of "template-free" or *de novo* production of RNA by the Qβ replicase (1) is important for our understanding of evolution because it involves the specific creation of genetic information by a protein enzyme. This would be in defiance of the central dogma of molecular biology (7) in which instruction flows only from nucleic acids to proteins. It is not surprising that the reported *de novo* production of RNA caused considerable controversy (8–12), as many molecular biologists saw contamination by RNA as the only possible explanation. Images recorded here demonstrate that a rapid process of evolution takes place, showing that it is natural selection that creates the specific self-replicating species of RNA. Since the RNA species acquire their only biological function of self-replication in the course of an experiment by changes in their nucleotide sequence, this process serves as a laboratory model of macroevolution, which is the irreversible evolution of new species with major functional and genetic change (13).

Spiegelmann's (14) *in vitro* experiments established microevolution of RNA templates. Chain initiation, elongation, and termination are retained in the simplest template-dependent chemical mechanism consistent with the kinetic data (4–6). However, the mechanism for template-free synthesis of RNA is not known. Self-replicating RNA molecules are produced *in vitro* in the enzyme solution within hours after the addition of NTP (1). Later, attempts were made to rationalize the phenomenon as contamination by RNA in the enzyme solution or from the air (10–12). Can the template-free synthesis be purified away or is it an exciting intrinsic property of the enzyme? Biebricher *et al.* (8, 9, 11) showed, using kinetic studies, that the mechanism of template-free synthesis must be very different from the well-understood template mechanism. The present work uses measurements of the probability distributions of reaction rates to show that the mechanism involves evolution.

Monitoring Evolution in Many Wave Fronts

Spatially extended replication reactions are motivated by Darwin's emphasis on the role of geographical isolation for evolution (15) and the requirement of compartmentalization for higher functional organization (16, 17). In one dimension, finite diffusion provides strong spatial isolation, so we were prompted to study molecular replication in a thin capillary filled with a solution containing the Qβ replicase, NTP monomers, and buffer. In the first experiments, localized amplification of RNA was established by injecting RNA templates at one location in the capillary. The presence of RNA could be monitored by increased fluorescence of the intercalating dye ethidium bromide (18). A region of enhanced fluorescence at the inoculation site appeared after a short lag, and this region grew in both directions for hours without weakening in intensity. These traveling waves show a constant velocity with a sharp transition profile in RNA concentration.

The RNA wave front velocity may be explicitly calculated in terms of the rate constants of the multicomponent template polymerization mechanism and the diffusion coefficients of the species involved (19). We demonstrated that the moving chemical wave front maintains a controlled exponentially growing phase in which selection of RNA takes place. The selective value of a molecular species is determined by its front velocity, calculated in the absence of competitors. In the usual case of high template–enzyme affinity, the front velocity is found (19) to have the Fisher form (20), $2\sqrt{\kappa D}$, where κ is the exponential-phase replication rate constant and D is the diffusion constant of the template–enzyme complex. In other cases, more complex expressions involving the rate coefficients and diffusion coefficients have been found (19), establishing the tractability of this form of inhomogeneous biochemistry for complex kinetics. Typically, the front velocity is on the order of 2 μm/sec or 0.5 cm/h. Measurements of front velocity have the advantage of being independent of the details of the sigmoidal fluorescence–RNA titration curve. Furthermore, the front velocity can be measured to within a fraction of a percent, providing unprecedented accuracy in the determination of selective value.

The publication costs of this article were defrayed in part by page charge payment. This article must therefore be hereby marked "*advertisement*" in accordance with 18 U.S.C. §1734 solely to indicate this fact.

*To whom reprint requests should be sent.
†Present address: BASF Aktiengesellschaft, D-6700 Ludwigshafen, F.R.G.

We designed an apparatus to investigate the stochastic nature of evolution (Fig. 1). Instead of RNA being injected at one location, RNA may be diluted to concentrations of <1 molecule per cm of capillary ($<10^{-16}$ M) so that the concentration waves initiated by single molecules may be measured after a stochastically varying lag period. The measurements at different locations are independent because of limited mass transfer by diffusion. This may be used to count molecules.

The spatially resolved fluorescence enhancement by RNA is recorded at regular time intervals by a CCD (charge-coupled device) camera. Image analysis is essential to reduce the data ($\approx 10^9$ fluorescence measurements per experiment) to evolutionary parameters. Space–time images of the one-dimensional fluorescence intensity along each of the ≈70 12-cm segments of the capillary summarize the time course of the replication reaction. These images, introduced in Fig. 2, may be analyzed as described in the legend to yield the appearance times, growth curves, and changing front velocities of up to 1700 distinct centers of replication in each experiment. The capillaries may be filled all together or in groups, the latter providing the opportunity to examine various reaction conditions in a single experiment. The results are stored in a PROLOG data base which currently contains kinetic information on about 70,000 replication reactions.

Wave Fronts from Single Molecules

Template-instructed kinetics of replication was investigated by filling capillaries with an enzyme solution (see Fig. 1) and

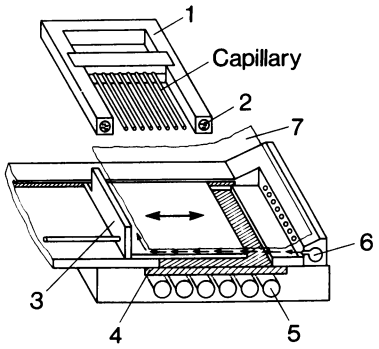

FIG. 1. Capillary reactor. A thin disposable polythene capillary (0.4 mm i.d. and ≈12 m long) is threaded back and forth on a steel frame (1) to produce a rectangular region with 70 parallel capillary segments each with an observable length of 12 cm. The frame is held at 30°C from within (2) by fluid pumped from a thermostat. It is mounted 5 mm above a filtered (4) UV (366 nm) transilluminator (5) [fitted with a piston-driven programmable shutter (3) with a 12 × 8 cm rectangular opening] and thermally insulated from the light source below by a UV-transparent sheet of plastic (7) cooled underneath by a stream of compressed air (6). The capillary was filled with ≈1 ml of the replicase solution [50 mM Tris·HCl (pH 7.5) containing 10% (wt/vol) glycerol, 10 mM dithiothreitol, 15 mM ethidium bromide, 8.5 mM $MgCl_2$, 0.5 mM NTP, 5 mM NaCl, and 0.5 μM holo Qβ replicase prepared as described (19), the last three concentrations being varied as described in the text; the $MgCl_2$ concentration varied with the NTP concentration C = 8 mM + [NTP], and in some cases small numbers of RNA molecules (in these experiments 86-nucleotide, MNV11; a gift from C. K. Biebricher) were added]. The capillary segments are sealed at the ends to avoid thermal expansion. Assembly of the capillary reactor and preparation of the template-free solutions were done in a separate room. Throughout the experiments, only disposables came into contact with the solutions. Pipetting devices were cleaned routinely by soaking in alkaline cleaning solution overnight and rinsing with prepacked HPLC water. The entire rectangular region is monitored through a narrow bandwidth red filter (FKG 14 510 nm), corresponding to the maximum wavelength of the RNA intercalation-enhanced fluorescence spectrum of ethidium bromide, by a Peltier cooled CCD (charge-coupled device) camera (1024 × 1024 pixel resolution) equipped with a 35-mm objective and programmable shutter.

concentrations of template down to an average of one RNA molecule per capillary. The RNA species used was MNV11, a single-stranded RNA of known sequence and length (87 nucleotides) (4). Titrations against template were performed in three single experiments at 5, 10, and 40 mM NaCl by filling groups of capillaries with each solution. Only 5% of the radioactively determined number of added templates initiated observable RNA traveling waves. We deal from here on with the effective number of molecules (= number/20). The first two titrations, shown in Fig. 3 *a–f*, covered a wide range of RNA molecules from 10 to 10^5 and from 100 to 2500 effective molecules per group. The third titration involved eight concentrations starting with 10 and increasing by factors of 2 to 1280 molecules per group. Spatially distinct centers of replication were observed up to the effective template concentrations along the capillary of 0.5 per mm.

The template titration allowed us to identify two classes of colonies: those proportional (in number) to the added templates (class I) and a background of colonies independent of the number of added templates (class II). The appearance times for colonies, determined by quadratic regression from the space–time pictures, are shown for four template concentrations in Fig. 4*A*. These lag times clearly separated colonies into the same two classes: (*i*) those appearing early with a narrow stochastic variation in lag times consistent with that of a linear birth process (class I) and (*ii*) those appearing late with a much wider scatter in lag times (class II). Front velocities in the template-dependent class I showed very narrow distributions compared with the broad distribution of velocities shown in Fig. 4*B* for the template-free class II. Individual measurements of front velocities were often to ±0.1%, sufficient to detect a small natural variation in the template-dependent front velocities.

The validity of the analytic formula for the front velocity has been experimentally tested. First, the predicted magnitude may be compared with experiment. Measured values of the exponential-phase rate coefficient (0.038 ± 0.002 s^{-1}) at 40 mM NaCl and the measured (3) diffusion constant for the replicase (0.38×10^{-6} $cm^2 \cdot s^{-1}$ corrected for viscosity) for the conditions of Fig. 4*A* give a predicted front velocity of $v = 2\sqrt{\kappa D} = 2.4$ μm/s. The corresponding average measured front velocity for template-induced replication of 0.82 cm/h or 2.28 μm/s agrees well with the predicted value.

Secondly, the known linear form of the dependence of replication time on the reciprocal NTP concentration for homogeneous reaction kinetics (typical of substrate dependencies for enzymatic reactions with Michaelis–Menton kinetics) may be compared with that obtained by measuring front velocities with the above formula. A Lineweaver–Burk plot using squared mean front velocities (instead of replication rate) with five NTP concentrations (1, 0.7, 0.5, 0.4, and 0.32 mM) proved linear, demonstrating in particular that $v \propto \kappa^{1/2}$, with an effective Michaelis constant of 1.3 ± 0.3 mM. This was similar to the value found for homogeneous kinetics under these reaction conditions, but a factor of 6 larger than that reported for Qβ viral RNA and MNV11 under different conditions (21, 22).

No significant variation of front velocity with enzyme concentration was found, consistent with the independence of homogeneous replication rate on enzyme concentration. Likewise, there is only a weak salt dependence of replication rates in homogeneous reactions involving MNV11. The lag times of the template-induced colonies showed little variation in the region containing a doubled salt concentration (10 mM NaCl) in Fig. 3 *a–c* (17 ± 2 min). This was confirmed by an additional experiment over the range from 5 to 40 mM.

Measurements of Nonseeded Wave Fronts

In contrast to the template-seeded colonies, the template-free colonies showed a pronounced shift to longer average lag

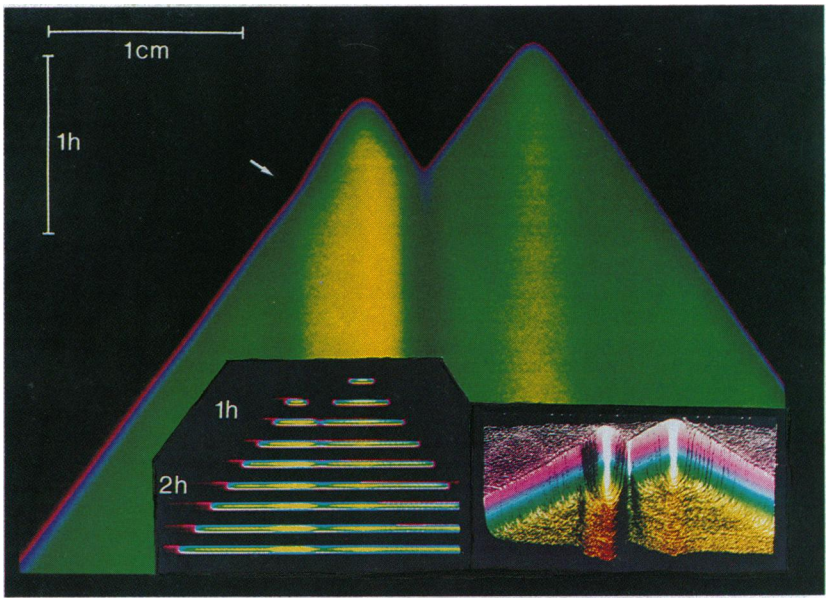

FIG. 2. Space-time image of replication waves. The image shows vertically the time course of RNA replication and spread in a short 5-cm segment of a capillary. The ethidium bromide fluorescence enhancement is a monotonic sigmoidal function of RNA concentration, so the graded colors represent increasing RNA concentrations from black to orange according to the scale shown in Fig. 2. A wave front of rapidly increasing RNA concentration propagates at constant velocity to the left and right of the positions where two single RNA molecules seeded the replication. A sharp increase in the front velocity (marked by the arrow) reflects a single evolutionary change in the replication rate of the RNA. (*Left inset*) A few of the hundreds of fluorescence enhancement images (t = 0 image subtracted) of the capillary segment at successive times that were used to reconstruct the space–time image. This was achieved by averaging laterally the fluorescence at each point along the capillary to form successive single horizontal rows of the image at successive times. The image is then filtered to remove the high-frequency noise that is constant in either the temporal or spatial direction. (*Right inset*) Three-dimensional character of the same space–time image shown by displaying the fluorescence intensity as depth in addition to color and using an imaginary sun to illuminate the surface from below. The solution in the capillary is as described in Fig. 1 but with 10 mM NaCl, 30 mM $(NH_4)_2SO_4$, 1 μM enzyme, and 3 μM ethidium bromide. The seeding RNA in this case was a nonoptimally replicating RNA (a cloned hybrid 133-nucleotide variant provided by C. Biebricher).

times at higher salt concentrations (29, 31, 35, and 45 min) in the experiment above. Fig. 3 *a–d* also shows a region with increased salt in which the average nonseeded lag times have increased (from 27 min at 5 mM to 40 min at 10 mM NaCl).

More dramatic is the difference with respect to the dependence on enzyme and NTP concentrations of lag times and front velocities for nonseeded as opposed to seeded RNA colonies. In two template-free experiments (at 22°C and 100 mM NaCl), the enzyme concentration was varied from 3.6 to 0.4 μM by using 10 regions of 13 capillaries each. The lag times ranged from a basal value of 6.5 h at high concentration to 20 h at 0.6 μM with no events recorded even after several days for 0.4 μM enzyme. Denaturation of the enzyme, with a half life of perhaps 10 h under these conditions, is the cause of the rapid fall off in the number of events at the lowest concentrations. The front velocities showed a broad distribution from 0.1 to 0.5 cm/h independent of enzyme concentration.

Varying NTP concentration from 12.5 mM to 0.32 mM (3.6 μM enzyme) in two further experiments (at 22°C and 100 mM NaCl) with template-free colonies produced a steady increase in lag times from 1.2 to 30 h. The distributions became steadily broader. Part of this data is shown in Fig. 4*B*. The front velocities had broad distributions with a maximum mean of 0.48 cm/h at 1.0 mM NTP, decreasing to just 0.13 cm/h at 0.32 mM. The decrease corresponds to a factor of >13 in the mean replication rate of RNA species for a 3-fold reduction in NTP concentration. The colonies differed widely not only in front velocities but also in their fluorescence intensities. Furthermore, a significant number of velocity changes were recorded in the template-independent colonies.

The above experiments with long lag times revealed strong evidence of major evolutionary changes in the RNA species in the course of time (Fig. 3 *g–i*). Front velocities of slowly growing species would increase in marked stages. Often, within a growing colony a secondary brightening of fluorescence starting at one point could be seen producing a new pair of traveling wave fronts growing inside the original colony (Fig. 3 *g* and *h*). When such a wave front reaches the boundary of the original colony, it may cause a sudden increase in the exterior front velocity of the colony. Sometimes a hierarchy of up to four such nested events is observed (Fig. 3*h*). In addition, most of the slower growing colonies have a weak fluorescence enhancement consistent with smaller concentrations resulting from high inactivation rates (e.g., by the annealing of templates to form nonreplicating double-stranded RNA). Fig. 3*i* shows the variety of behavior after collision of wave fronts from different colonies. In particular, increases in front velocity correlated with two wave-front collisions appear to be frequent. This provides suggestive evidence for recombination of RNA in this single enzyme system.

Discussion

Traditionally, biochemists have taken great pains to avoid spatially inhomogeneous reactions. The present work makes use of the simplification of small concentrations in the leading tail of a traveling concentration wave, providing a constant exponential-growth-phase dilution reactor with kinetics simply related to the ideal homogeneous case. Because the reactor involves no moving parts, a scale up to thousands of wave fronts in a single experiment using only 1 ml of solution proved possible.

The above results show how the spontaneous generation of RNA in nonseeded colonies is a stochastic process with very different statistics from the simpler amplification process from single template molecules. The latter is quite well described by a simple birth process based on the deterministic kinetic mechanism established at high concentrations. The template-free colonies exhibit a very different mean kinetics and have a much greater variation in front velocities and lag times. The images of Fig. 3 *g–i* show that the cause of these differences in stochastic behavior is that the formation of template-free RNA colonies involves a major process of evolution. We have characterized the intrinsic phenotypic variation in replication rate arising from this process (e.g., see Fig. 4*B*) and its dependence on reaction conditions.

The direct observation of ubiquitous evolutionary succession in *de novo* colonies confirms the many indirect arguments against a contamination cause. Of course the fact that these experiments were carried out in sealed capillaries with template-free colonies forming as late as after 2 days of incubation rules out contamination through the air (12). The template-free reaction may only be observed when the reaction mix is free of contaminants (see Fig. 1 legend) and the concentrations of reactants, in particular the enzyme and monomers, are in the appropriate range. One outstanding

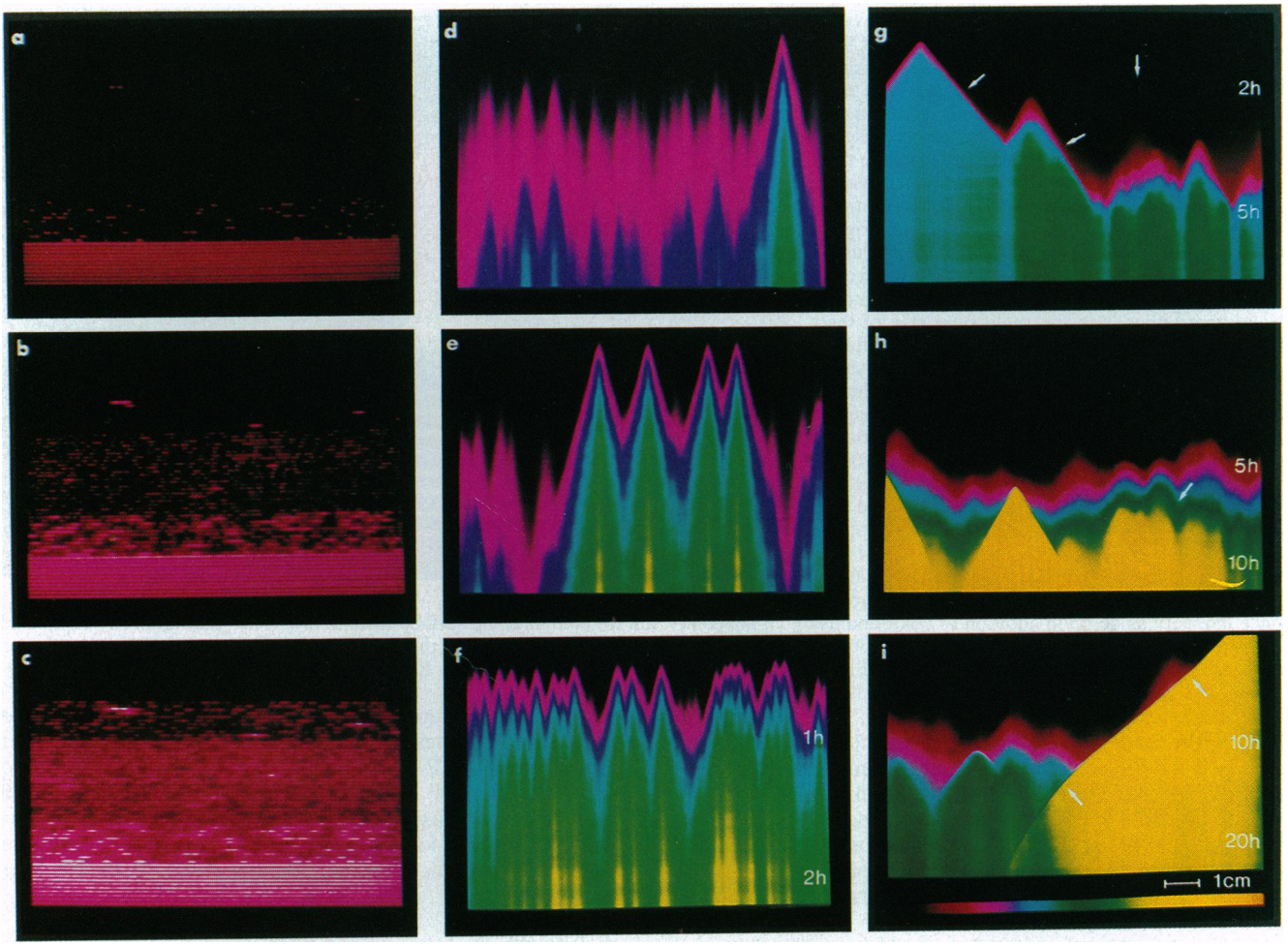

FIG. 3. Seeded and spontaneous RNA replication waves. (*a–c*) Spatially resolved fluorescence images at three successive times (22, 31, and 45 min) of waves in 66 capillaries. The lower four regions of these six 11-capillary rectangular regions contain increasing numbers of RNA template molecules: 10, 100, 1000, and 10^5 per region. A second class of waves independent of the number of templates may be seen. The top two regions show 100 templates in two other biochemical environments—lower replicase activity and increased salt (10 mM NaCl). The fluorescence intensity color scale and distance scale are shown in *i*. (*d–f*) Space–time images with increasing numbers of templates: addition of 100, 500, and 2500 strands of RNA in the three capillaries of each image. Image *d* is of capillary no. 14 from the experiment in *a–c*, whereas *e* and *f* follow capillaries from a separate experiment under identical conditions (10 mM NaCl; see Fig. 1). (*g–i*) Evolution in *de novo* RNA replication waves. Three space–time images are shown of capillaries without added RNA template, under reaction conditions where replication waves appear up to 1 day. Image *g* shows the marked variation in velocity and appearance times of *de novo* replication waves (slanted arrows) and the initiation of new waves within a weakly growing RNA species (vertical arrow). In *h*, the hierarchy of successively brighter colonies (arrow) is most likely associated with mutants with a decreased inactivation rate by double-strand formation. In *i*, the RNA species growing from the right undergoes a sudden increase in front velocity as it meets and grows through and beyond another more weakly fluorescent one (right arrow). This suggests some form of recombination between the two RNA species involved. In this case, the resultant species can invade a region filled with other *de novo* products (left arrow). The reaction conditions were as described in Fig. 1 but with (*i*) the following concentration changes for *g*: 10 mM NaCl, 30 mM $(NH_4)_2SO_4$, 1 μM enzyme, and 3 μM ethidium bromide; and (*ii*) the change of temperature to 22°C for *h* and *i* and the following concentration changes: 100 mM NaCl (*h* and *i*), 3.6 μM enzyme (*h* and *i*), and 0.7 mM (*h*) and 0.5 mM (*i*) NTP.

question is why only about 5% of the RNA molecules form colonies.

The evolutionary interpretation of the above findings is corroborated by product analyses of the RNA resulting from these template-free reactions after long incubation. Gel electrophoresis had shown some of the slowly replicating RNA to be about 40 nucleotides long, shorter by a factor of 2 or more than the final optimized products (80–140 nucleotides). Short RNA molecules as short as 25 nucleotides have been isolated from the *de novo* reaction and sequenced by DNA amplification (23). The appearance of widely differing sequences not only demonstrates that self-replication may be achieved with very different sequences but also makes contamination unlikely as a cause of *de novo* RNA. If RNA contamination were the cause, one would expect the sequences to reflect the dominant replicating species in the laboratory, which they do not.

A process of random copolymerization, generating the first replicator, followed by natural selection would explain both the different sequences found in independent *de novo* reactions and the sequence homogeneity of individual *de novo* populations. Of course, the transition from random synthesis to replication may involve an intermediate stage of partial instruction, and the initially "random" synthesis may be constrained significantly by the replicase.

This means, however, that here is an ideal model system for studying evolutionary change. The rapid increase in the size of our data base will no doubt provoke the attention of evolutionary theorists. As a result of the high population numbers compared with the reciprocal of the error rate (3×10^{-4}) (24, 25) and with the length of the RNA sequence, the concept of species must be replaced here by that of quasi-species (26): the multiple-error mutants of the wild-type RNA sequence compose a significant fraction of any stationary

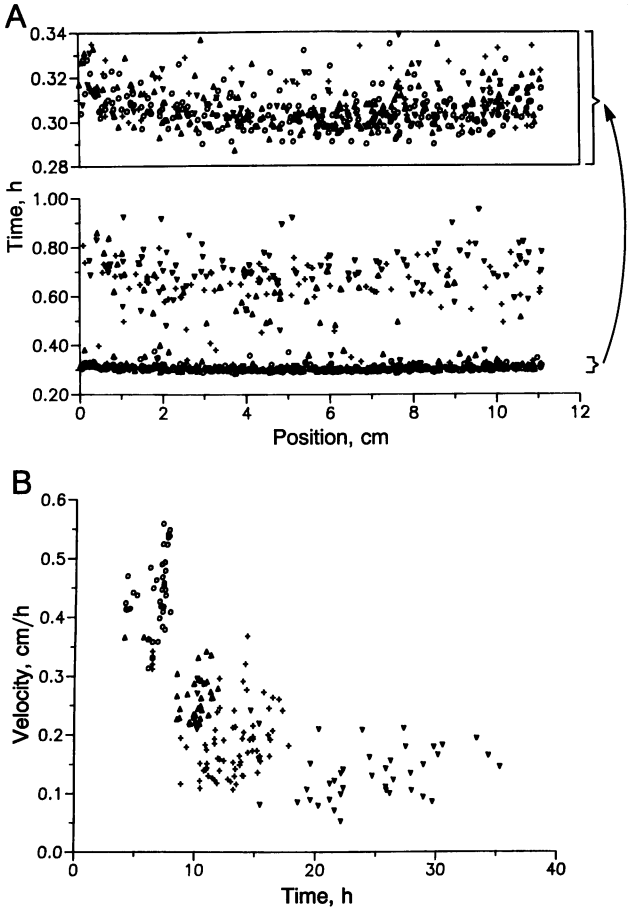

FIG. 4. RNA front velocities and appearance times. Representative data is shown from the analysis of replication waves recorded in the space–time images of single experiments. (*A*) Appearance times of distinct RNA colonies with four different effective RNA inoculation numbers (128, 64, 32, and 16) of molecules per capillary in 40 mM NaCl. The appearance times separate into two classes: class I, early appearance with a standard deviation on the order of 2 doubling times, and class II, much later appearance and more disperse. (*B*) *de novo* velocities vs. colony appearance time for four concentrations of NTP (0.7, 0.5, 0.4, and 0.32 mM). At an intensity value corresponding to an RNA concentration in the late exponential phase of growth, a contour of time vs. position is established to subpixel accuracy by vertical (time axis) linear interpolation of the intensities in each filtered space–time image. An optimal piecewise linear fit of the contours is performed by using the *t* statistic at 95% confidence in an iterated search over all remaining position subintervals to determine the one with the most significant regression line. Regression on the resulting line segments give the front velocities along with error bounds. The appearance times and positions of the start of each spatially distinct molecular colony are determined by quadratic regression to the contour in the vicinity of the boundaries between segments of opposite slope.

RNA population and codetermine the fitness of the wild type. One nonobvious consequence is that sequence fixation may occur with an arbitrarily small superiority in replication rate (27, 28). Recent work on viruses such as influenza and human immunodeficiency virus (29, 30) have demonstrated the practical importance of quasi-species theory.

In summary, we have monitored major evolutionary changes in the replicating RNA that was formed without added template. This evolution concerns the acquisition of perhaps the most basic phenotypic property—replication rate. The events may be monitored in sufficient frequency and accuracy to allow a clear stochastic characterization. Experiments with other isothermal genetic amplification systems are needed. The authors anticipate that further *de novo* sequence "instruction" processes will be found in other enzymic systems that provide the prerequisites for natural selection. The DNA-dependent T7 RNA polymerase may be such a candidate (8). The Qβ case demonstrates just how much natural selection can look like teleological instruction if the time scale of evolution is made short enough.

The authors are thankful for excellent laboratory assistance by S. Völker. M. Meyer and R. Oberdieck assisted with the photographic reproduction and technical drawing. J. Yin made valuable suggestions concerning the presentation. Likewise, numerous discussions with C. K. Biebricher and the support of M. Eigen are gratefully acknowledged.

1. Sumper, M. & Luce, R. (1975) *Proc. Natl. Acad. Sci. USA* **72,** 162–166.
2. Weissmann, C., Billeter, M. A., Goodman, H. M., Hindley, J. & Weber, H. A. (1973) *Annu. Rev. Biochem.* **42,** 303–328.
3. Blumenthal, T. & Carmichael, G. G. (1979) *Annu. Rev. Biochem.* **48,** 525–548.
4. Biebricher, C. K., Eigen, M. & Gardiner, W. C., Jr. (1983) *Biochemistry* **22,** 2544–2559.
5. Biebricher, C. K., Eigen, M. & Gardiner, W. C., Jr. (1984) *Biochemistry* **23,** 3186–3194.
6. Biebricher, C. K., Eigen, M. & Gardiner, W. C., Jr. (1985) *Biochemistry* **24,** 6550–6560.
7. Watson, J. D. & Crick, F. H. C. (1953) *Nature (London)* **171,** 737–738.
8. Biebricher, C. K., Eigen, M. & Luce, R. (1981) *J. Mol. Biol.* **148,** 369–390.
9. Biebricher, C. K., Eigen, M. & Luce, R. (1981) *J. Mol. Biol.* **148,** 391–410.
10. Hill, D. & Blumenthal, T. (1983) *Nature (London)* **301,** 350–352.
11. Biebricher, C. K., Eigen, M. & Luce, R. (1986) *Nature (London)* **321,** 89–91.
12. Chetverin, B. A., Chetverin, H. V. & Munishkin, A. V. (1991) *J. Mol. Biol.* **222,** 3–9.
13. Dobzhansky, T. (1970) *Genetics of the Evolutionary Process* (Columbia Univ. Press, New York), p. 429.
14. Mills, D. R., Peterson, R. L. & Spiegelmann, S. (1967) *Proc. Natl. Acad. Sci. USA* **58,** 217–224.
15. Darwin, C. (1859) *The Origin of Species by Means of Natural Selection* (Murray, London).
16. Eigen, M. (1971) *Naturwissenschaften* **58,** 465–523.
17. Niesert, U., Harnasch, D. & Bresch, C. (1981) *J. Mol. Evol.* **17,** 348–353.
18. Le Pecq, J. B. & Paoletti, C. (1971) *Methods Biochem. Anal.* **20,** 41–86.
19. Bauer, G. J., McCaskill, J. S. & Otten, H. (1989) *Proc. Natl. Acad. Sci. USA* **86,** 7937–7941.
20. Fisher, R. A. (1937) *Ann. Eugen.* **7,** 355–369.
21. Mitsunari, Y. & Hori, K. (1973) *J. Biochem.* **74,** 263–271.
22. Biebricher, C. K., Eigen, M. & Luce, R. (1981) *J. Mol. Biol.* **148,** 391–410.
23. Biebricher, C. K. & Luce, R. (1992) *Adv. Space Res.* **12,** 191–197.
24. Batschelet, E., Domingo, E. & Weissmann, C. (1976) *Gene* **1,** 27–32.
25. Domingo, E., Sabo, D., Taniguchi, T. & Weissmann, C. (1978) *Cell* **13,** 735–744.
26. Eigen, M., McCaskill, J. S. & Schuster, P. (1989) *Adv. Chem. Phys.* **75,** 149–263.
27. McCaskill, J. S. (1984) *J. Chem. Phys.* **80,** 5194–5202.
28. Chao, L. (1990) *Nature (London)* **348,** 454–455.
29. Nee, S. & Maynard Smith, J. (1990) *Parasitology* **100,** S5–S18.
30. Nowak, M., May, R. M. & Anderson, R. M. (1990) *AIDS* **4,** 1095–1103.
31. Konarska, M. M. & Sharp, P. A. (1990) *Cell* **63,** 609–618.